Meccanica (2011) 46: 75–88
DOI 10.1007/s11012-010-9390-0

PARALLEL MANIPULATORS

Comparison of 3-RPR planar parallel manipulators with regard to their kinetostatic performance and sensitivity to geometric uncertainties

Nicolas Binaud · Stéphane Caro · Philippe Wenger

Received: 20 September 2009 / Accepted: 15 November 2010 / Published online: 2 December 2010
© Springer Science+Business Media B.V. 2010

Abstract This paper deals with the sensitivity analysis of 3-RPR planar parallel manipulators. First, the manipulators under study as well as their degeneracy conditions are presented. Then, an optimization problem is formulated in order to obtain their maximal regular dexterous workspace. Moreover, the sensitivity coefficients of the pose of the manipulator moving platform to variations in the geometric parameters and in the actuated variables are expressed algebraically. Two aggregate sensitivity indices are determined, one related to the orientation of the manipulator moving platform and another one related to its position. Then, we compare two non-degenerate and two degenerate 3-RPR planar parallel manipulators with regard to their dexterity, workspace size and sensitivity. Finally, two actuating modes are compared with regard to their sensitivity.

Keywords Sensitivity analysis · Degenerate manipulators · Regular dextrous workspace · Transmission angle

N. Binaud · S. Caro (✉) · P. Wenger
UMR CNRS n° 6597, Institut de Recherche en Communications et Cybernétique de Nantes, 1 rue de la Noë, 44321 Nantes, France
e-mail: caro@irccyn.ec-nantes.fr

N. Binaud
e-mail: binaud@irccyn.ec-nantes.fr

P. Wenger
e-mail: wenger@irccyn.ec-nantes.fr

1 Introduction

Variations in the geometric parameters of PKMs can be either compensated or amplified. For that reason, it is important to analyze the sensitivity of the mechanism performance to variations in its geometric parameters. For instance, Wang et al. [1] studied the effect of manufacturing tolerances on the accuracy of a Stewart platform. Kim et al. [2] used a forward error bound analysis to find the error bound of the end-effector of a Stewart platform when the error bounds of the joints are given, and an inverse error bound analysis to determine those of the joints for the given error bound of the end-effector. Kim and Tsai [3] studied the effect of misalignment of linear actuators of a 3-Degree of Freedom (DOF) translational parallel manipulator on the motion of its moving platform. Caro et al. [4] developed a tolerance synthesis method for mechanisms based on a robust design approach. Cardou et al. [5] proposed some kinematic-sensitivity indices for dimensionally nonhomogeneous Jacobian matrices. Caro et al. [6] proposed two indices to evaluate the sensitivity of the end-effector pose (position + orientation) of Orthoglide 3-axis, a 3-DOF translational PKM, to variations in its design parameters. Besides, they noticed that the better the dexterity, the higher the accuracy of the manipulator. However, Yu et al. [7] claimed that the accuracy of a 3-DOF Planar Parallel Manipulator (PPM) is not necessarily related to its dexterity. Meng et al. [8] proposed a method to analyze the accuracy of parallel manipulators with

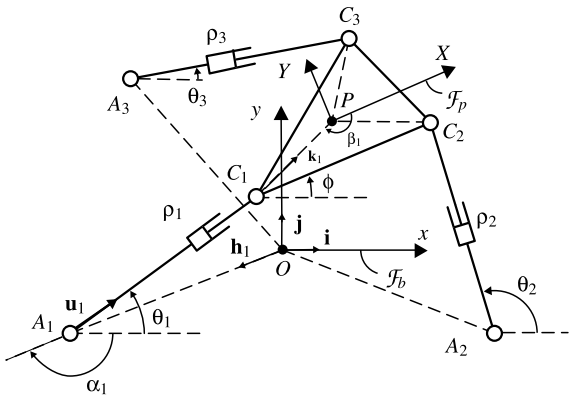

Fig. 1 3-RPR manipulator

joint clearances and ended up with a standard convex optimization problem to evaluate the maximal pose error in a prescribed workspace.

Some architectures of planar parallel manipulators are compared with regard to their sensitivity to geometric uncertainties in [9].

This paper deals with the comparison of the sensitivity of two degenerate and two non-degenerate 3-RPR PPMs. Likewise, the sensitivity of two actuating modes of the 3-RPR PPM, namely the 3-RPR PPM and the 3-RPR PPM, is analyzed. First, the degeneracy conditions of 3-RPR manipulators and the manipulators under study are presented. Then, the formulation of an optimization problem is introduced to obtain the regular dexterous workspace of those manipulators. Finally, a methodology is introduced to analyze and compare the sensitivity of the pose of their moving platforms to variations in their geometric parameters.

2 Manipulator architecture

Here and throughout this paper, R, P and P denote revolute, prismatic and actuated prismatic joints, respectively. Figure 1 illustrates the architecture of the manipulator under study. It is composed of a base and a moving platform (MP) connected with three legs. Points A_1, A_2 and A_3, (C_1, C_2 and C_3, respectively) lie at the corners of a triangle, of which point O (point P, resp.) is the circumcenter. Each leg is composed of a R, a P and a R joints in sequence. The three P joints are actuated. Accordingly, the manipulator is named 3-RPR manipulator.

$\mathcal{F}_b$ and $\mathcal{F}_p$ are the base and the moving platform frames of the manipulator. In the scope of this paper, $\mathcal{F}_b$ and $\mathcal{F}_p$ are supposed to be orthogonal. $\mathcal{F}_b$ is defined with the orthogonal dihedron $(\vec{O}x, \vec{O}y)$, point O being its center and $\vec{O}x$ parallel to segment A_1A_2. Likewise, $\mathcal{F}_p$ is defined with the orthogonal dihedron $(\vec{P}X, \vec{P}Y)$, point C being its center and $\vec{P}X$ parallel to segment C_1C_2.

The pose of the manipulator MP, i.e., its position and its orientation, is determined by means of the Cartesian coordinates vector $\mathbf{p} = [p_x, p_y]^T$ of operation point P expressed in frame $\mathcal{F}_b$ and angle ϕ, that is the angle between frames $\mathcal{F}_b$ and $\mathcal{F}_p$. Finally, the passive joints do not have any stop.

3 Degenerate and non-degenerate manipulators

In this section, we focus on the sensitivity analysis of two degenerate and two non-degenerate 3-RPR manipulators. First, the degeneracy conditions of such manipulators are given. Then, the architectures of the four manipulators under study are illustrated.

3.1 Degeneracy condition

The forward kinematic problem of a parallel manipulator often leads to complex equations and non analytic solutions, even when considering 3-DOF PPMs [10]. For those manipulators, Hunt showed that the forward kinematics admits at most six solutions [11] and some authors proved that their forward kinematics can be reduced to the solution of a sixth-degree characteristic polynomial [12, 13].

As shown in [14, 15] and [16], a 3-RPR PPM is said to be degenerate when the degree of its characteristic polynomial becomes smaller than six. Six types of degenerate 3-RPR PPMs exists in the literature, namely,

1. 3-RPR PPMs with two coincident joints;
2. 3-RPR PPMs with similar aligned base and moving platforms;
3. 3-RPR PPMs with nonsimilar aligned base and moving platforms;
4. 3-RPR PPMs with similar triangular base and moving platforms;
5. 3-RPR PPMs with the three actuated prismatic joints satisfying a certain relationship;
6. 3-RPR PPMs with congruent base and moving platforms, of which the moving platform is rotated of 180 deg about one of its side.

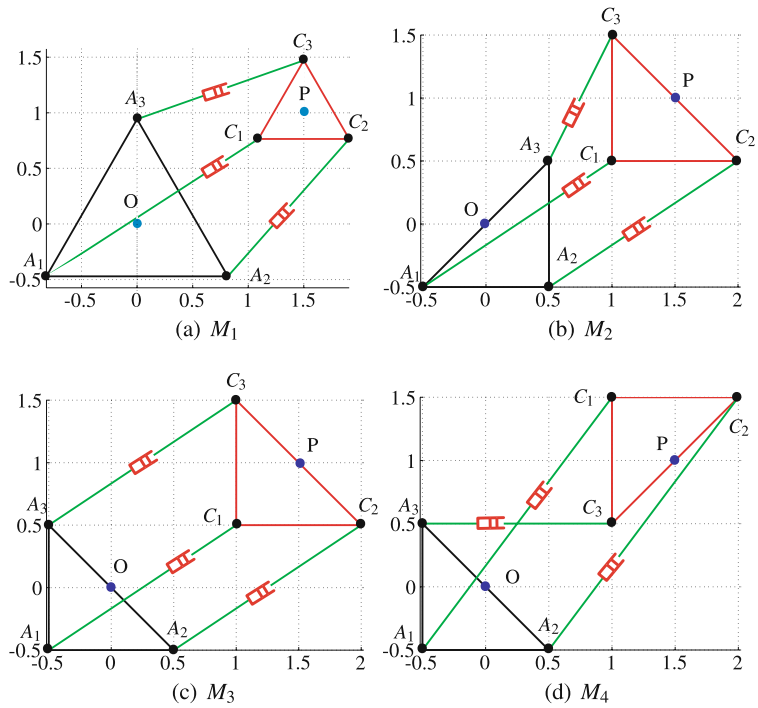

Fig. 2 The four 3-RPR manipulators under study with $\phi = 0$ and $\mathbf{p} = [1, 1.5]^T$: (**a**)–(**b**) non-degenerate manipulators, (**c**)–(**d**) degenerate manipulators

In the scope of this paper, we focus on the sensitivity analysis of the fourth and the sixth cases. For the fourth case, the forward kinematics is reduced to the solution of two quadratics in cascade. For the sixth case, the forward kinematics degenerates over the whole joint space and is reduced to the solution of a third-degree polynomial and a quadratic in sequence.

3.2 Manipulators under study

Figures 2(a)–(d) illustrate the four manipulators under study, named M_1, M_2, M_3 and M_4, respectively. M_1 and M_2 are non-degenerate manipulators while M_3 and M_4 are degenerate manipulators. From Fig. 2(a), the base and moving platforms of M_1 are equilateral. From Fig. 2(b), the base and moving platforms of M_2 are identical but in a different geometric configuration for an orientation $\phi = 0$. M_3 and M_4 illustrate the fourth and the sixth degeneracy cases presented in Sect. 3.1. It is noteworthy that the base and moving platforms of M_2, M_3 and M_4 have the same circumscribed circle, its radius being equal to $\sqrt{2}/2$. As far as M_1 is concerned, the circumscribed circle of its moving platform is two times smaller than the one of the base platform.

To compare the sensitivity of these PPMs, the geometric parameters have to be normalized. Therefore, let R_1 and R_2 be the radii of the base and moving platforms of the PPM. In order to come up with finite values, R_1 and R_2 are normalized as in [17–19]. For that matter, let N_f be a normalizing factor:

$$N_f = (R_1 + R_2)/2 \tag{1}$$

and

$$r_m = R_m/N_f, \quad m = 1, 2 \tag{2}$$

Therefore,

$$r_1 + r_2 = 2 \tag{3}$$

From (2) and (3), we can notice that:

$$r_1 \in [0, 2], \qquad r_2 \in [0, 2] \tag{4}$$

As the former two-dimensional infinite space corresponding to geometric parameters R_1 and R_2 is reduced to a one-dimensional finite space defined with

(3), the workspace analysis of the 3-RPR manipulator under study turns out to be easier.

4 Regular dexterous workspace

In order to compare the sensitivity of the foregoing manipulators, we first define their Regular Dexterous Workspace (RDW). Then, the sensitivity of M_1, M_2, M_3 and M_4 can be evaluated throughout their RDW and compared. The RDW of a manipulator is a regular-shaped part of its workspace with good and homogeneous kinetostatic performance. The shape of the RDW is up to the designer. It may be a cube, a parallelepiped, a cylinder or another regular shape. A good shape fits to the singular surfaces.

The kinetostatic performance of a manipulator is usually characterized by the conditioning number of its kinematic Jacobian matrix [20, 21]. From [22, 23], the transmission angle of a 3-DOF PPM can be also used to evaluate its kinetostatic performance. Here, we prefer to use the transmission angle as a kinetostatic performance index as it does not require the normalization of the kinematic Jacobian matrix. On the contrary, the kinematic Jacobian matrix of 3-DOF PPM has to be normalized by means of a normalizing length in order its conditioning number to make sense [24].

4.1 Transmission angle

The transmission angle ψ_i associated with the ith leg is defined as the angle between force vector $\mathbf{Fc}_i$ and translational velocity vector $\mathbf{Vc}_i$ at point C_i as illustrated in Fig. 3.

The direction of force $\mathbf{Fc}_i$ is the direction of leg A_iC_i, namely,

$$\gamma_i = \arctan\left(\frac{y_{C_i} - y_{A_i}}{x_{C_i} - x_{A_i}}\right), \quad i = 1, 2, 3 \tag{5}$$

The instantaneous centre of rotation depends on the leg under study. For example, instantaneous centre of rotation I_1 associated with leg 1 is the intersecting point of forces $\mathbf{Fc}_2$ anf $\mathbf{Fc}_3$.

Table 1 gives the Cartesian coordinates of instantaneous centre of rotation I_i associated with the ith leg of the 3-RPR PPM, expressed in frame $\mathcal{F}_b$, with $b_i = y_{C_i} - x_{C_i}\tan\gamma_i$, $i = 1, 2, 3$.

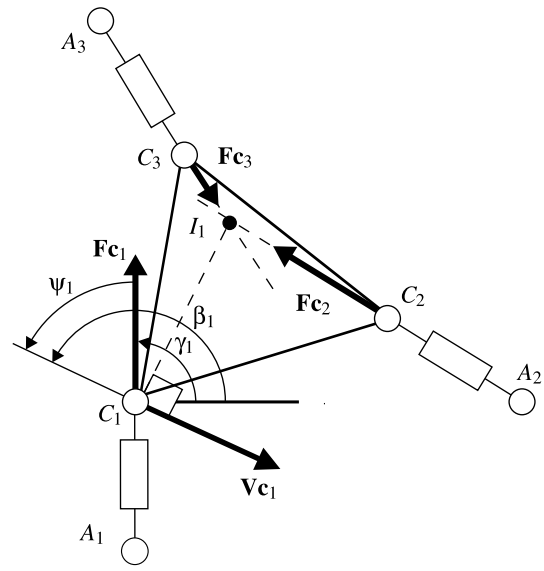

Fig. 3 Transmission angle of the 3-RPR PPMs

The direction of $\mathbf{Vc}_i$ is defined as,

$$\beta_i = \arctan\left(\frac{y_{C_i} - y_{I_i}}{x_{C_i} - x_{I_i}}\right) + \frac{\pi}{2}, \quad i = 1, 2, 3 \tag{6}$$

Accordingly,

$$\psi_i = |\gamma_i - \beta_i|, \quad i = 1, 2, 3 \tag{7}$$

Finally, the transmission angle ψ of the overall mechanism is defined as,

$$\psi = \max(\psi_i), \quad i = 1, 2, 3 \tag{8}$$

and the smaller ψ, the better the force transmission of the mechanism.

4.2 RDW determination

In the scope of this study, the RDW of the PPM is supposed to be a cylinder of ϕ-axis with good kinetostatic performance, i.e., the transmission angle ψ is smaller than 75° throughout the cylinder. In order to obtain such a RDW, we can solve the following optimization problem:

$$Pb \left| \begin{array}{ll} \min\limits_{\mathbf{x}} & 1/R \\ \text{s.t.} & \Delta\phi \geq 30^\circ \\ & \psi \leq 75^\circ \end{array} \right.$$

Table 1 Cartesian coordinates of instantaneous centres of rotation

	I_1	I_2	I_3
x_{I_i}	$\frac{b_3-b_2}{\tan(\gamma_2)-\tan(\gamma_3)}$	$\frac{b_1-b_3}{\tan(\gamma_3)-\tan(\gamma_1)}$	$\frac{b_2-b_1}{\tan(\gamma_1)-\tan(\gamma_2)}$
y_{I_i}	$\frac{b_3\tan(\gamma_2)-b_2\tan(\gamma_3)}{\tan(\gamma_2)-\tan(\gamma_3)}$	$\frac{b_1\tan(\gamma_3)-b_3\tan(\gamma_1)}{\tan(\gamma_3)-\tan(\gamma_1)}$	$\frac{b_2\tan(\gamma_1)-b_1\tan(\gamma_2)}{\tan(\gamma_1)-\tan(\gamma_2)}$

Table 2 RDW radius of M_1, M_2, M_3 and M_4

R_1	R_2	R_3	R_4
1.21	0.62	0.75	2.69

R being the radius of the cylinder and $\Delta\phi$ the orientation range of the MP of the manipulator within its RDW. Here, $\Delta\phi$ is equal to 30° arbitrarily. This optimization problem has five decision variables:

$$\mathbf{x} = \begin{bmatrix} R & I_x & I_y & \phi_{min} & \phi_{max} \end{bmatrix}$$

I_x and I_y being the Cartesian coordinates of the center of the cylinder, ϕ_{min} and ϕ_{max} being the lower and upper bounds of ϕ angle ($\Delta\phi = \phi_{max} - \phi_{min}$).

This optimization problem is solved by means of a Tabu search Hooke and Jeeves algorithm [25]. As a result, the RDW of the manipulator is completely defined by means of the decision variables corresponding to the global minimum.[1]

Figures 4(d) illustrate the workspace, the singularities and the maximal RDW of M_1, M_2, M_3 and M_4. Their radii are given in Table 2. We can notice that M_4 has the biggest RDW and M_2 the smallest one.

5 Sensitivity analysis

In this section, the sensitivity of M_1, M_2, M_3 and M_4 is evaluated throughout their RDW for a matter of comparison. The sensitivity coefficients, and, two aggregate sensitivity indices are determined to analyze the sensitivity of the pose of the moving platform of a 3-RPR manipulator to variations in its geometric parameters. Then, the contours of these indices are plotted in M_1, M_2, M_3 and M_4 RDWs and the results are analyzed.

[1]The solution obtained with a Tabu search Hooke and Jeeves algorithm will not be necessarily the global optimum. However, it will provide a solution that is close to the global one and satisfactory in the framework of this research work.

5.1 Sensitivity coefficients

From the closed-loop kinematic chains $O - A_i - C_i - P - O$, $i = 1, \ldots, 3$ depicted in Fig. 1, the position vector $\mathbf{p}$ of point P can be expressed in $\mathcal{F}_b$ as follows,

$$\mathbf{p} = \begin{bmatrix} p_x \\ p_y \end{bmatrix} = \mathbf{a}_i + (\mathbf{c}_i - \mathbf{a}_i) + (\mathbf{p} - \mathbf{c}_i), \quad i = 1, \ldots, 3 \tag{9}$$

$\mathbf{a}_i$ and $\mathbf{c}_i$ being the position vectors of points A_i and C_i expressed in $\mathcal{F}_b$. Equation (9) can also be written as,

$$\mathbf{p} = a_i \mathbf{h}_i + \rho_i \mathbf{u}_i + c_i \mathbf{k}_i \tag{10}$$

with

$$\mathbf{h}_i = \begin{bmatrix} \cos\alpha_i \\ \sin\alpha_i \end{bmatrix}, \qquad \mathbf{u}_i = \begin{bmatrix} \cos\theta_i \\ \sin\theta_i \end{bmatrix},$$

$$\mathbf{k}_i = \begin{bmatrix} \cos(\phi + \beta_i + \pi) \\ \sin(\phi + \beta_i + \pi) \end{bmatrix}$$

where a_i is the distance between points O and A_i, ρ_i is the distance between points A_i and C_i, c_i is the distance between points C_i and P, $\mathbf{h}_i$ is the unit vector $\vec{OA_i}/\|\vec{OA_i}\|_2$, $\mathbf{u}_i$ is the unit vector $\vec{A_iC_i}/\|\vec{A_iC_i}\|_2$ and $\mathbf{k}_i$ is the unit vector $\vec{C_iP}/\|\vec{C_iP}\|_2$.

Upon differentiation of (10), we obtain:

$$\delta\mathbf{p} = \delta a_i\, \mathbf{h}_i + a_i\, \delta\alpha_i\, \mathbf{E}\,\mathbf{h}_i + \delta\rho_i\, \mathbf{u}_i + \rho_i\, \delta\theta_i\, \mathbf{E}\,\mathbf{u}_i + \delta c_i\, \mathbf{k}_i + c_i\, (\delta\phi + \delta\beta_i)\, \mathbf{E}\,\mathbf{k}_i \tag{11}$$

with matrix $\mathbf{E}$ defined as

$$\mathbf{E} = \begin{bmatrix} 0 & -1 \\ 1 & 0 \end{bmatrix} \tag{12}$$

$\delta\mathbf{p}$ and $\delta\phi$ being the position and orientation errors of the MP. Likewise, δa_i, $\delta\alpha_i$, $\delta\rho_i$, δc_i and $\delta\beta_i$ denote the variations in a_i, α_i, ρ_i, c_i and β_i, respectively.

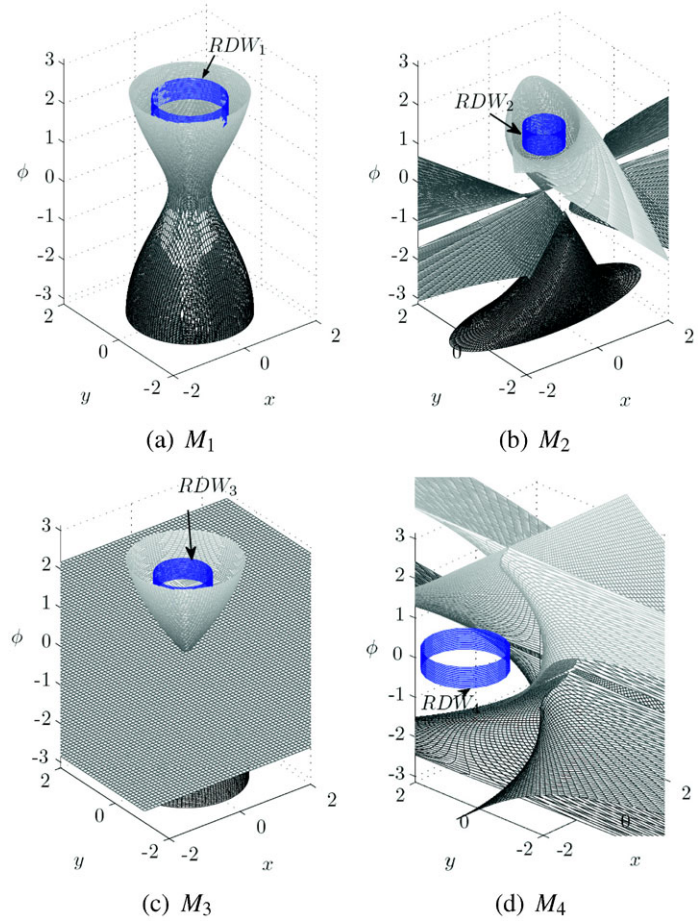

Fig. 4 Maximal regular dexterous workspace

The idle variation $\delta\theta_i$ is eliminated by dot-multiplying (11) by $\rho_i \mathbf{u}_i^T$, thus obtaining

$$\rho_i\,\mathbf{u}_i^T\,\delta\mathbf{p} = \rho_i\,\delta a_i\,\mathbf{u}_i^T\mathbf{h}_i + \rho_i\,a_i\,\delta\alpha_i\,\mathbf{u}_i^T\mathbf{E}\mathbf{h}_i + \rho_i\,\delta\rho_i + \rho_i\,\delta c_i\,\mathbf{u}_i^T\mathbf{k}_i + \rho_i\,c_i\,(\delta\phi + \delta\beta_i)\,\mathbf{u}_i^T\mathbf{E}\mathbf{k}_i \tag{13}$$

Equation (13) can now be cast in vector form, namely,

$$\mathbf{A}\begin{bmatrix}\delta\phi\\ \delta\mathbf{p}\end{bmatrix} = \mathbf{H}_a\begin{bmatrix}\delta a_1\\ \delta a_2\\ \delta a_3\end{bmatrix} + \mathbf{H}_\alpha\begin{bmatrix}\delta\alpha_1\\ \delta\alpha_2\\ \delta\alpha_3\end{bmatrix} + \mathbf{B}\begin{bmatrix}\delta\rho_1\\ \delta\rho_2\\ \delta\rho_3\end{bmatrix} + \mathbf{H}_c\begin{bmatrix}\delta c_1\\ \delta c_2\\ \delta c_3\end{bmatrix} + \mathbf{H}_\beta\begin{bmatrix}\delta\beta_1\\ \delta\beta_2\\ \delta\beta_3\end{bmatrix} \tag{14}$$

with

$$\mathbf{A} = \begin{bmatrix} m_1 & \rho_1\mathbf{u}_1^T\\ m_2 & \rho_2\mathbf{u}_2^T\\ m_3 & \rho_3\mathbf{u}_3^T\end{bmatrix}, \qquad \mathbf{B} = \begin{bmatrix}\rho_1 & 0 & 0\\ 0 & \rho_2 & 0\\ 0 & 0 & \rho_3\end{bmatrix} \tag{15a}$$

$$\mathbf{H}_a = \operatorname{diag}\left[\rho_1\mathbf{u}_1^T\mathbf{h}_1 \quad \rho_2\mathbf{u}_2^T\mathbf{h}_2 \quad \rho_3\mathbf{u}_3^T\mathbf{h}_3\right] \tag{15b}$$

$$\mathbf{H}_\alpha = \operatorname{diag}\left[\rho_1 a_1\mathbf{u}_1^T\mathbf{E}\mathbf{h}_1 \quad \rho_2 a_2\mathbf{u}_2^T\mathbf{E}\mathbf{h}_2 \quad \rho_3 a_3\mathbf{u}_3^T\mathbf{E}\mathbf{h}_3\right] \tag{15c}$$

$$\mathbf{H}_c = \operatorname{diag}\left[\rho_1\mathbf{u}_1^T\mathbf{k}_1 \quad \rho_2\mathbf{u}_2^T\mathbf{k}_2 \quad \rho_3\mathbf{u}_3^T\mathbf{k}_3\right] \tag{15d}$$

$$\mathbf{H}_\beta = \operatorname{diag}\left[\rho_1 c_1\mathbf{u}_1^T\mathbf{E}\mathbf{k}_1 \quad \rho_2 c_2\mathbf{u}_2^T\mathbf{E}\mathbf{k}_2 \quad \rho_3 c_3\mathbf{u}_3^T\mathbf{E}\mathbf{k}_3\right] \tag{15e}$$

and

$$m_i = -\rho_i\,c_i\,\mathbf{u}_i^T\mathbf{E}\mathbf{k}_i, \quad i = 1,\ldots,3 \tag{16}$$

Let us notice that $\mathbf{A}$ and $\mathbf{B}$ are the direct and the inverse Jacobian matrices of the manipulator, respectively. Assuming that $\mathbf{A}$ is non singular, i.e., the manipulator does not meet any Type II singularity [26], we obtain upon multiplication of (14) by $\mathbf{A}^{-1}$:

$$\begin{bmatrix}\delta\phi\\ \delta\mathbf{p}\end{bmatrix} = \mathbf{J}_a\begin{bmatrix}\delta a_1\\ \delta a_2\\ \delta a_3\end{bmatrix} + \mathbf{J}_\alpha\begin{bmatrix}\delta\alpha_1\\ \delta\alpha_2\\ \delta\alpha_3\end{bmatrix} + \mathbf{J}\begin{bmatrix}\delta\rho_1\\ \delta\rho_2\\ \delta\rho_3\end{bmatrix} + \mathbf{J}_c\begin{bmatrix}\delta c_1\\ \delta c_2\\ \delta c_3\end{bmatrix} + \mathbf{J}_\beta\begin{bmatrix}\delta\beta_1\\ \delta\beta_2\\ \delta\beta_3\end{bmatrix} \tag{17}$$

with

$$\mathbf{J} = \mathbf{A}^{-1}\mathbf{B} \tag{18a}$$

$$\mathbf{J}_a = \mathbf{A}^{-1}\mathbf{H}_a \tag{18b}$$

$$\mathbf{J}_\alpha = \mathbf{A}^{-1}\mathbf{H}_\alpha \tag{18c}$$

$$\mathbf{J}_c = \mathbf{A}^{-1}\mathbf{H}_c \tag{18d}$$

$$\mathbf{J}_\beta = \mathbf{A}^{-1}\mathbf{H}_\beta \tag{18e}$$

and

$$\mathbf{A}^{-1} = \frac{1}{\det(\mathbf{A})}\begin{bmatrix}v_1 & v_2 & v_3\\ \mathbf{v}_1 & \mathbf{v}_2 & \mathbf{v}_3\end{bmatrix} \tag{19a}$$

$$v_i = \rho_j\rho_k(\mathbf{u}_j\times\mathbf{u}_k)^T\mathbf{k} \tag{19b}$$

$$\mathbf{v}_i = \mathbf{E}\left(m_j\rho_k\mathbf{u}_k - m_k\rho_j\mathbf{u}_j\right) \tag{19c}$$

$$\det(\mathbf{A}) = \sum_{i=1}^{3} m_i v_i \tag{19d}$$

$$\mathbf{k} = \mathbf{i}\times\mathbf{j} \tag{19e}$$

$j = (i+1)$ modulo 3; $k = (i+2)$ modulo 3; $i = 1,2,3$. $\mathbf{J}$ is the kinematic Jacobian matrix of the manipulator whereas $\mathbf{J}_a$, $\mathbf{J}_\alpha$, $\mathbf{J}_c$ and $\mathbf{J}_\beta$ are named *sensitivity Jacobian matrices* of the pose of the MP to variations in a_i, α_i, c_i and β_i, respectively. Indeed, the terms of $\mathbf{J}_a$, $\mathbf{J}_\alpha$, $\mathbf{J}_c$ and $\mathbf{J}_\beta$ are the sensitivity coefficients of the position and the orientation of the moving platform of the manipulator to variations in the Polar coordinates of points A_i and C_i. Likewise, $\mathbf{J}$ contains the sensitivity coefficients of the pose of the MP of the manipulator to variations in the prismatic actuated joints. It is noteworthy that all these sensitivity coefficients are expressed algebraically.

Let δa_{ix} and δa_{iy} denote the position errors of points A_i, $i = 1,2,3$, along $\vec{O}x$ and $\vec{O}y$, namely, the variations in the Cartesian coordinates of points A_i. Likewise, let δc_{iX} and δc_{iY} denote the position errors of points C_i along $\vec{P}X$ and $\vec{P}Y$, namely, the variations in the Cartesian coordinates of points C_i.

From Fig. 1,

$$\begin{bmatrix}\delta a_{ix}\\ \delta a_{iy}\end{bmatrix} = \begin{bmatrix}\cos\alpha_i & -a_i\sin\alpha_i\\ \sin\alpha_i & a_i\cos\alpha_i\end{bmatrix}\begin{bmatrix}\delta a_i\\ \delta\alpha_i\end{bmatrix} \tag{20a}$$

$$\begin{bmatrix}\delta c_{iX}\\ \delta c_{iY}\end{bmatrix} = \begin{bmatrix}\cos\beta_i & -c_i\sin\beta_i\\ \sin\beta_i & c_i\cos\beta_i\end{bmatrix}\begin{bmatrix}\delta c_i\\ \delta\beta_i\end{bmatrix} \tag{20b}$$

Accordingly, from (17) and (20a)–(20b), we obtain the following relation between the pose error of the MP and variations in the Cartesian coordinates of points A_i and C_i:

$$\begin{bmatrix}\delta\phi\\ \delta\mathbf{p}\end{bmatrix} = \mathbf{J}_A\begin{bmatrix}\delta a_{1x}\\ \delta a_{1y}\\ \delta a_{2x}\\ \delta a_{2y}\\ \delta a_{3x}\\ \delta a_{3y}\end{bmatrix} + \mathbf{J}\begin{bmatrix}\delta\rho_1\\ \delta\rho_2\\ \delta\rho_3\end{bmatrix} + \mathbf{J}_C\begin{bmatrix}\delta c_{1X}\\ \delta c_{1Y}\\ \delta c_{2X}\\ \delta c_{2Y}\\ \delta c_{3X}\\ \delta c_{3Y}\end{bmatrix} \tag{21}$$

$\mathbf{J}_A$ and $\mathbf{J}_C$ being named *sensitivity Jacobian matrices* of the pose of the MP to variations in the Cartesian coordinates of points A_i and C_i, respectively. Indeed, the terms of $\mathbf{J}_A$ and $\mathbf{J}_C$ are the sensitivity coefficients of the pose of the MP to variations in the Cartesian coordinates of points A_i and C_i.

In order to better highlight the sensitivity coefficients, let us write the 3×6 matrices $\mathbf{J}_A$ and $\mathbf{J}_C$ and the 3×3 matrix $\mathbf{J}$ as follows:

$$\mathbf{J}_A = \begin{bmatrix}\mathbf{J}_{A_1} & \mathbf{J}_{A_2} & \mathbf{J}_{A_3}\end{bmatrix} \tag{22a}$$

$$\mathbf{J}_C = \begin{bmatrix}\mathbf{J}_{C_1} & \mathbf{J}_{C_2} & \mathbf{J}_{C_3}\end{bmatrix} \tag{22b}$$

$$\mathbf{J} = \begin{bmatrix}\mathbf{j}_1 & \mathbf{j}_2 & \mathbf{j}_3\end{bmatrix} \tag{22c}$$

the 3×2 matrices $\mathbf{J}_{A_i}$ and $\mathbf{J}_{C_i}$ and the three dimensional vectors $\mathbf{j}_i$ being expressed as:

$$\mathbf{J}_{A_i} = \begin{bmatrix}\mathbf{j}_{A_i\phi}\\ \mathbf{J}_{A_i p}\end{bmatrix}, \quad i = 1,2,3 \tag{23a}$$

$$\mathbf{J}_{C_i} = \begin{bmatrix}\mathbf{j}_{C_i\phi}\\ \mathbf{J}_{C_i p}\end{bmatrix}, \quad i = 1,2,3 \tag{23b}$$

$$\mathbf{j}_i = \begin{bmatrix}j_{i\phi}\\ \mathbf{j}_{ip}\end{bmatrix}, \quad i = 1,2,3 \tag{23c}$$

with

$$\mathbf{j}_{A_i\phi} = \frac{1}{\det(\mathbf{A})}\begin{bmatrix} v_i\, q_i & v_i\, r_i \end{bmatrix} \tag{24a}$$

$$\mathbf{j}_{C_i\phi} = \frac{1}{\det(\mathbf{A})}\begin{bmatrix} v_i\, s_i & v_i\, t_i \end{bmatrix} \tag{24b}$$

$$j_{i\phi} = \frac{\rho_i\, v_i}{\det(\mathbf{A})} \tag{24c}$$

$$\mathbf{J}_{A_i p} = \frac{1}{\det(\mathbf{A})}\begin{bmatrix} q_i\mathbf{v}_i^T\mathbf{i} & r_i\mathbf{v}_i^T\mathbf{i} \\ q_i\mathbf{v}_i^T\mathbf{j} & r_i\mathbf{v}_i^T\mathbf{j} \end{bmatrix} \tag{24d}$$

$$\mathbf{J}_{C_i p} = \frac{1}{\det(\mathbf{A})}\begin{bmatrix} s_i\mathbf{v}_i^T\mathbf{i} & t_i\mathbf{v}_i^T\mathbf{i} \\ s_i\mathbf{v}_i^T\mathbf{j} & t_i\mathbf{v}_i^T\mathbf{j} \end{bmatrix} \tag{24e}$$

$$\mathbf{j}_{ip} = \frac{1}{\det(\mathbf{A})}\begin{bmatrix} \rho_i\mathbf{v}_i^T\mathbf{i} \\ \rho_i\mathbf{v}_i^T\mathbf{j} \end{bmatrix} \tag{24f}$$

q_i, r_i, s_i and t_i taking the form:

$$q_i = \rho_i\mathbf{u}_i^T\mathbf{i} \tag{25a}$$

$$r_i = \rho_i\mathbf{u}_i^T\mathbf{j} \tag{25b}$$

$$s_i = \rho_i\mathbf{u}_i^T\mathbf{k}_i\cos\beta_i - \rho_i\mathbf{u}_i^T\mathbf{E}\mathbf{k}_i\sin\beta_i \tag{25c}$$

$$t_i = \rho_i\mathbf{u}_i^T\mathbf{k}_i\sin\beta_i + \rho_i\mathbf{u}_i^T\mathbf{E}\mathbf{k}_i\cos\beta_i \tag{25d}$$

$\mathbf{j}_{A_i\phi}, \mathbf{j}_{C_i\phi}$ and $j_{i\phi}$ contain the sensitivity coefficients of the orientation of the MP of the manipulator to variations in the Cartesian coordinates of points A_i, C_i and prismatic actuated variables, respectively. Similarly, $\mathbf{J}_{A_i p}$, $\mathbf{J}_{C_i p}$ and $\mathbf{j}_{ip}$ contain the sensitivity coefficients related to the position of the MP.

Accordingly, the designer of such a planar parallel manipulator can easily identify the most influential geometric variations to the pose of its MP and synthesize proper dimensional tolerances from the previous sensitivity coefficients. Two aggregate sensitivity indices related to the geometric errors of the moving and base platforms are introduced thereafter.

5.2 Global sensitivity indices

The pose errors of the manipulator MP depend on variations in the geometric parameters as well as on the

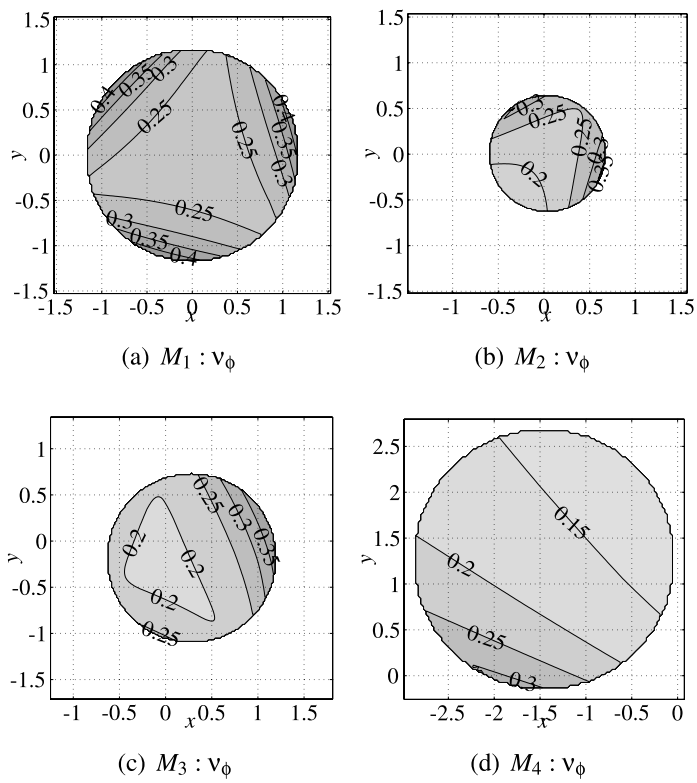

Fig. 5 ν_ϕ isocontours of: (**a**) M_1, (**b**) M_2, (**c**) M_3 and (**d**) M_4

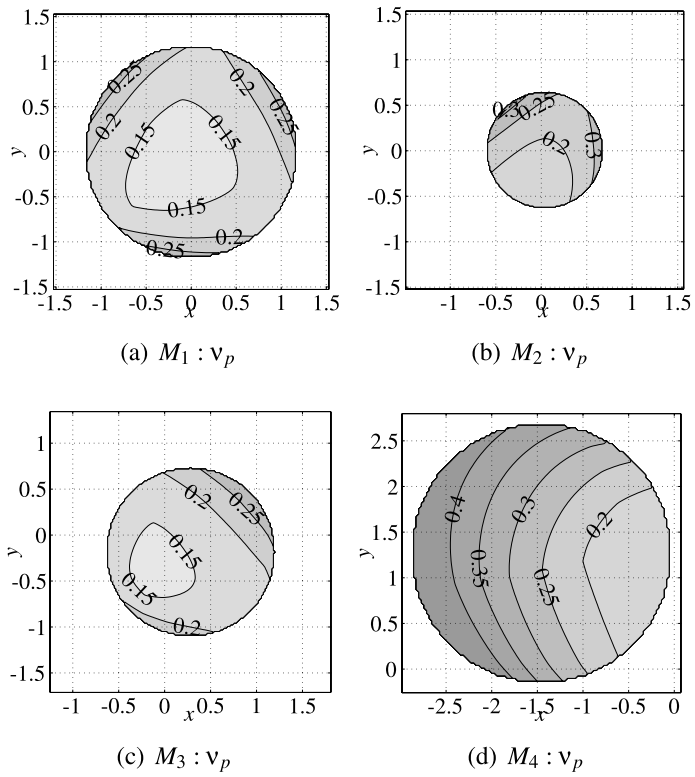

Fig. 6 ν_p isocontours of: (**a**) M_1, (**b**) M_2, (**c**) M_3 and (**d**) M_4

Table 3 Values of $\overline{\nu_\phi}$, $\nu_{\phi_{max}}$, $\overline{\nu_p}$ and $\nu_{p_{max}}$ for M_1, M_2, M_3 and M_4

	M_1	M_2	M_3	M_4
$\overline{\nu_\phi}$	0.292	0.254	0.233	0.192
$\nu_{\phi_{max}}$	0.426	0.365	0.386	0.322
$\overline{\nu_p}$	0.171	0.231	0.194	0.316
$\nu_{p_{max}}$	0.263	0.327	0.284	0.441

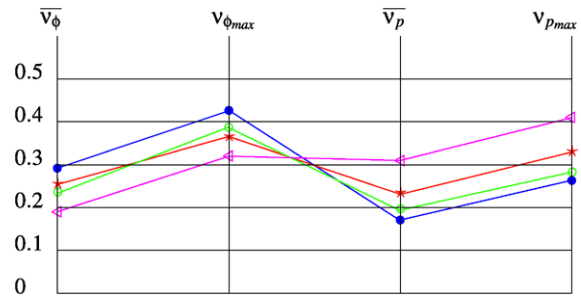

Fig. 7 Comparison of ●—●: M_1, ⋆—⋆: M_2, ○—○: M_3, ◁—◁: M_4

manipulator configuration. In order to analyze the influence of the manipulator configuration on those errors, let us first formulate some indices in order to assess the aggregate sensitivity of the MP pose to variations in the geometric parameters for a given manipulator configuration. To this end, let (21) be expressed as:

$$\begin{bmatrix} \delta\phi \\ \delta\mathbf{p} \end{bmatrix} = \mathbf{J}_s \begin{bmatrix} \delta\mathbf{a_i} & \delta\rho_\mathbf{i} & \delta\mathbf{c_i} \end{bmatrix}^T \tag{26}$$

with

$$\mathbf{J}_s = \begin{bmatrix} \mathbf{J}_A & \mathbf{J} & \mathbf{J}_C \end{bmatrix} \tag{27}$$

and

$$\delta\mathbf{a_i} = \begin{bmatrix} \delta a_{1x} & \delta a_{1y} & \delta a_{2x} & \delta a_{2y} & \delta a_{3x} & \delta a_{3y} \end{bmatrix} \tag{28a}$$

$$\delta\rho_\mathbf{i} = \begin{bmatrix} \delta\rho_1 & \delta\rho_2 & \delta\rho_3 \end{bmatrix} \tag{28b}$$

$$\delta\mathbf{c_i} = \begin{bmatrix} \delta c_{1X} & \delta c_{1Y} & \delta c_{2X} & \delta c_{2Y} & \delta c_{3X} & \delta c_{3Y} \end{bmatrix} \tag{28c}$$

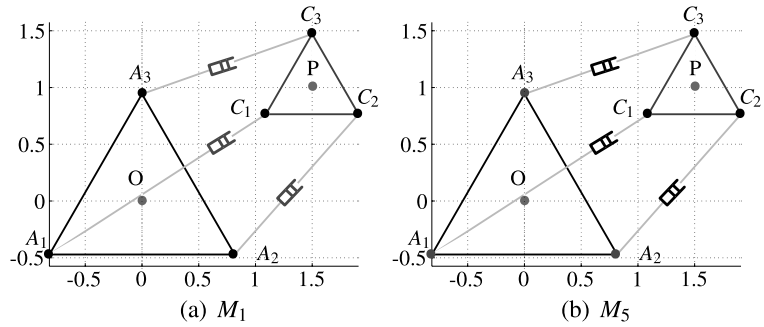

(a) M_1 (b) M_5

Fig. 8 Two actuating modes: (**a**) 3-RPR manipulator, (**b**) 3-RPR manipulator, $\phi = 0$ and $\mathbf{p} = [1.5, 1]^T$

Table 4 The eight actuating modes of the 3-RPR PPM

Actuating mode number		active angles
1	$\underline{R}PR_1$-$\underline{R}PR_2$-$\underline{R}PR_3$	$\theta_1, \theta_2, \theta_3$
2	$\underline{R}PR_1$-$\underline{R}PR_2$-$R\underline{P}R_3$	$\theta_1, \theta_2, \rho_3$
3	$\underline{R}PR_1$-$R\underline{P}R_2$-$\underline{R}PR_3$	$\theta_1, \rho_2, \theta_3$
4	$R\underline{P}R_1$-$\underline{R}PR_2$-$\underline{R}PR_3$	$\rho_1, \theta_2, \theta_3$
5	$\underline{R}PR_1$-$R\underline{P}R_2$-$R\underline{P}R_3$	θ_1, ρ_2, ρ_3
6	$R\underline{P}R_1$-$R\underline{P}R_2$-$\underline{R}PR_3$	ρ_1, ρ_2, θ_3
7	$R\underline{P}R_1$-$\underline{R}PR_2$-$R\underline{P}R_3$	ρ_1, θ_2, ρ_3
8	$R\underline{P}R_1$-$R\underline{P}R_2$-$R\underline{P}R_3$	ρ_1, ρ_2, ρ_3

Table 5 RDW radius of M_1 and M_5

R_1	R_5
1.21	1.60

The 3×15 matrix $\mathbf{J}_s$ is named "sensitivity Jacobian matrix" and can be written as follows:

$$\mathbf{J}_s = \begin{bmatrix} \mathbf{j}_{s\phi} \\ \mathbf{J}_{sp} \end{bmatrix} \tag{29}$$

with

$$\mathbf{j}_{s\phi} = [\,\mathbf{j}_{A_1\phi} \quad \mathbf{j}_{A_2\phi} \quad \mathbf{j}_{A_3\phi} \quad j_{1\phi} \quad j_{2\phi} \quad j_{3\phi} \quad \mathbf{j}_{C_1\phi} \quad \mathbf{j}_{C_2\phi} \quad \mathbf{j}_{C_3\phi}\,] \tag{30a}$$

$$\mathbf{J}_{s_p} = [\,\mathbf{J}_{A_1p} \quad \mathbf{J}_{A_2p} \quad \mathbf{J}_{A_3p} \quad \mathbf{j}_{1p} \quad \mathbf{j}_{2p} \quad \mathbf{j}_{3p} \quad \mathbf{J}_{C_1p} \quad \mathbf{J}_{C_2p} \quad \mathbf{J}_{C_3p}\,] \tag{30b}$$

From (30a), we can define an aggregate sensitivity index ν_ϕ of the orientation of the MP of the manipulator to variations in its geometric parameters and prismatic actuated joints, namely,

Table 6 Values of $\overline{\nu_\phi}$, $\nu_{\phi max}$, $\overline{\nu_p}$ and ν_{pmax} for M_1 and M_5

	M_1	M_5
$\overline{\nu_\phi}$	0.251	0.289
$\nu_{\phi_{max}}$	0.448	0.501
$\overline{\nu_p}$	0.163	0.222
$\nu_{p_{max}}$	0.369	0.423

$$\nu_\phi = \frac{\|\mathbf{j}_{s_\phi}\|_2}{n_v} \tag{31}$$

n_v being the number of variations that are considered. Here, n_v is equal to 15.

Likewise, from (30b), an aggregate sensitivity index ν_p of the position of the MP of the manipulator to variations in its geometric parameters and prismatic actuated joints can be defined as follows:

$$\nu_p = \frac{\|\mathbf{J}_{s_p}\|_2}{n_v} \tag{32}$$

For any given manipulator configuration, the lower ν_ϕ, the lower the overall sensitivity of the orientation of its MP to variations in the geometric parameters. Similarly, the lower ν_p, the lower the overall sensitivity of the MP position to variations in the geometric parameters. As a matter of fact, ν_ϕ (ν_p, resp.) characterizes the intrinsic sensitivity of the MP orientation (position, resp.) to any variation in the geometric parameters. Let us notice that ν_p as well as the sensitivity coefficients related to the MP position defined in Sects. 5.1 are frame dependent, whereas ν_ϕ and the sensitivity coefficients related to the MP orientation are not.

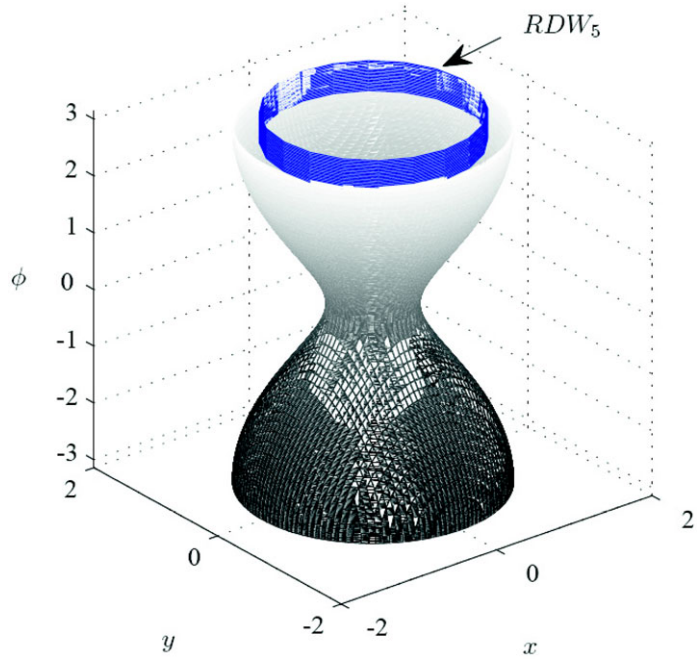

Fig. 9 M_5 regular dexterous workspace

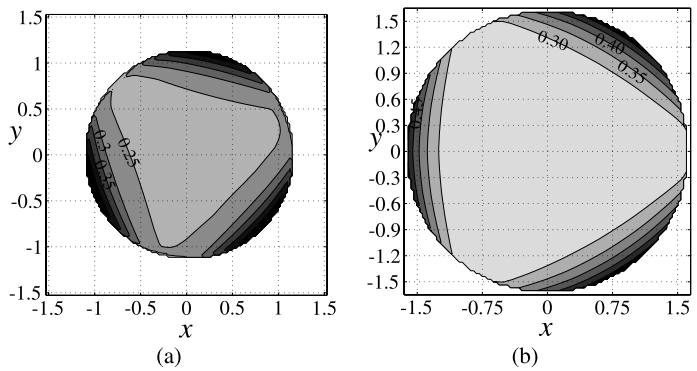

Fig. 10 (**a**) M_1 ν_ϕ and (**b**) M_5 ν_ϕ isocontours

In order to evaluate the sensitivity of the manipulator over its workspace or part of it, four global sensitivity indices are defined as follows:

$$\overline{\nu_\phi} = \frac{\int_W \nu_\phi \, \mathrm{d}W}{\int_W \mathrm{d}W} \tag{33a}$$

$$\nu_{\phi_{max}} = \max(\nu_\phi) \tag{33b}$$

$$\overline{\nu_p} = \frac{\int_W \nu_p \, \mathrm{d}W}{\int_W \mathrm{d}W} \tag{33c}$$

$$\nu_{p_{max}} = \max(\nu_p) \tag{33d}$$

$\overline{\nu_\phi}$ and $\overline{\nu_p}$ are the average values of ν_ϕ and ν_p over W, W being the manipulator workspace or part of it. Likewise, $\nu_{\phi_{max}}$ and $\nu_{p_{max}}$ are the maximum values of ν_ϕ and ν_p over W.

Finally, ν_ϕ, $\overline{\nu_\phi}$ and $\nu_{\phi_{max}}$ are expressed in [rad/L], whereas ν_p, $\overline{\nu_p}$ and $\nu_{p_{max}}$ are dimensionless, [L] being the unit of length.

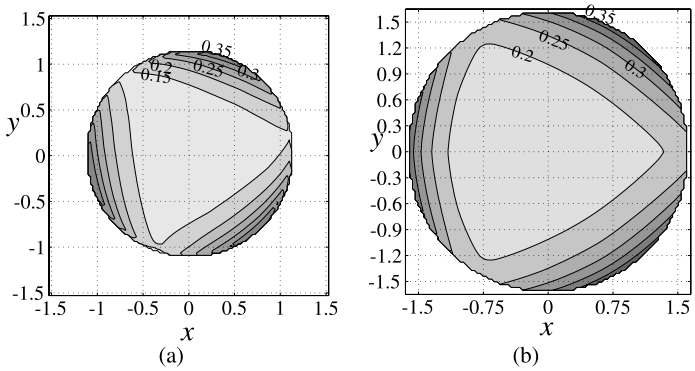

Fig. 11 (**a**) M_1 ν_p and (**b**) M_5 ν_p isocontours

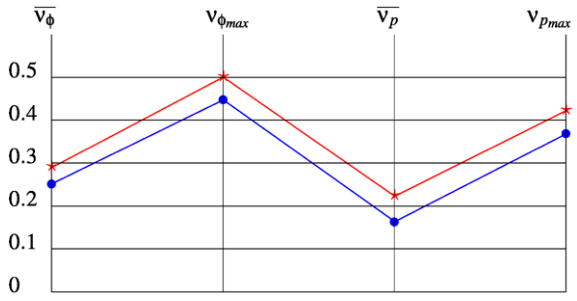

Fig. 12 Comparison of ●—●: M_1 and ⋆—⋆: M_5

5.3 Comparison of two non-degenerate and two degenerate 3-RPR PPMs

In this section, the sensitivity of M_1, M_2, M_3 and M_4 is evaluated within their RDW for a matter of comparison based on aggregate sensitivity indices ν_ϕ and ν_p defined in (31) and (32) and global sensitivity indices $\overline{\nu_\phi}$, $\nu_{\phi_{max}}$, $\overline{\nu_p}$ and $\nu_{p_{max}}$ defined in (33a)–(33d).

Figures 5(a)–(d) (Figs. 6(a)–(d), resp.) illustrate the isocontours of the maximum value of ν_ϕ (ν_p, resp.). for a given orientation ϕ of the MP throughout the RDW of M_1, M_2, M_3 and M_4, respectively.

Table 3 and Fig. 7 illustrate the values of $\overline{\nu_\phi}$, $\nu_{\phi_{max}}$, $\overline{\nu_p}$ and $\nu_{p_{max}}$ for the four manipulators under study. It is apparent that M_4 has the least sensitive orientation of its MP and that M_1 has the least sensitive position of its MP. On the contrary, M_4 has the most sensitive position of its MP and M_1 has the most sensitive orientation of its MP.

6 Sensitivity comparison of two actuating modes

In this section, two actuating modes of the 3-RPR PPM, namely the 3-RPR PPM and the 3-RPR PPM, are compared with regard to their sensitivity to variations in geometric parameters.[2]

Table 4 shows the eight actuating modes of the 3-RPR PPM. For instance, the first actuating mode corresponds to the 3-RPR PPM, also called $\underline{R}PR_1$-$\underline{R}PR_2$-$\underline{R}PR_3$ PPM in the scope of this paper, as the first revolute joints (located at points A_i) of its limbs are actuated. Likewise, the eighth actuating mode corresponds to the 3-RPR PPM, also called $R\underline{P}R_1$-$R\underline{P}R_2$-$R\underline{P}R_3$ PPM, as the prismatic joints of its limbs are actuated. For the fourth actuating mode, the prismatic joint of the first limb is actuated while the first revolute joints of the two other limbs are actuated.

Let M_1 and M_5 denote the 3-RPR and the 3-RPR PPMs, respectively, as shown in Figs. 8(a)–(b). The RDW of M_5 is illustrated in Fig. 9. From Table 5, we can notice that the RDW of M_5 is larger than the one of M_1.

Figures 10(a)–(b) show the isocontours of the maximum value of $\nu_{\phi M_1}$ and $\nu_{\phi M_5}$ throughout the RDW of M_1 and M_5. Likewise, Figs. 11(a)–(b) show the isocontours of the maximum value of ν_{pM_1} and ν_{pM_5}. As a matter of fact, those isocontours correspond to the maximal global positioning and orientation errors with

[2] As the actuators are not of the same type for the two manipulators (revolute actuators for the first one and prismatic actuators of the second one), their variations are not considered in order the sensitivity comparison of the two manipulators to make sense.

regard to the orientation ϕ of the moving platform of the manipulator.

Table 6 and Fig. 12 illustrate the values of $\overline{\nu_\phi}$, $\nu_{\phi_{max}}$, $\overline{\nu_p}$ and $\nu_{p_{max}}$ for the two actuating modes under study. It is apparent that M_1 is better than M_5, both in terms of orientation and positioning errors of its moving platform due to variations in geometric parameters.

7 Conclusions

This paper dealt with the sensitivity analysis of 3-RPR planar parallel manipulators (PPMs). First, the manipulators under study as well as their degeneracy conditions were presented. Then, an optimization problem was formulated in order to obtain their maximal regular dexterous workspace (RDW). Accordingly, the sensitivity of the pose of their moving platform to variations in geometric parameters was evaluated within their RDW. Then, a methodology was proposed to compare PPMs with regard to their dexterity and sensitivity. Four 3-RPR PPMs were compared as illustrative examples. Moreover, two actuating modes were compared with regard to their sensitivity to geometric uncertainties. Finally, four global sensitivity indices were introduced in order to evaluate the sensitivity of PPMs over their Cartesian workspace. Those indices characterize the intrinsic sensitivity of the moving platform pose to any variation in the geometric parameters. They are like amplification factors of errors in geometric parameters. There values remain always lower than one for the manipulators under study. It means that there is no amplification of errors in geometric parameters. The proposed indices can also be used to help the designer of PPMs select a good manipulator architecture at the conceptual design stage.

References

1. Wang J, Masory O (1993) On the accuracy of a Stewart platform—Part I, The effect of manufacturing tolerances. In: Proceedings of the IEEE international conference on robotics automation, ICRA'93, Atlanta, USA, pp 114–120
2. Kim HS, Choi YJ (2000) The kinematic error bound analysis of the Stewart platform. J Robot Syst 17:63–73
3. Kim HS, Tsai L-W (2003) Design optimization of a Cartesian parallel manipulator. ASME J Mech Des 125:43–51
4. Caro S, Bennis F, Wenger P (2005) Tolerance synthesis of mechanisms: A robust design approach. ASME J Mech Des 127:86–94
5. Cardou P, Bouchard S, Gosselin C (2010) Kinematic-sensitivity indices for dimensionally nonhomogeneous Jacobian matrices. IEEE Trans Robot 26(1):166–173
6. Caro S, Wenger P, Bennis F, Chablat D (2006) Sensitivity analysis of the orthoglide, A 3-DOF translational parallel kinematic machine. ASME J Mech Des 128:392–402
7. Yu A, Bonev IA, Zsombor-Murray PJ (2007) Geometric method for the accuracy analysis of a class of 3-DOF planar parallel robots. Mech Mach Theory 43(3):364–375
8. Meng J, Zhang D, Li Z (2009) Accuracy analysis of parallel manipulators with joint clearance. ASME J Mech Des 131:011013
9. Binaud N, Caro S, Wenger P (2010) Sensitivity comparison of planar parallel manipulators. Mech Mach Theory 45:1477–1490
10. Hunt KH (1978) Kinematic geometry of mechanisms. Oxford University Press, Cambridge
11. Hunt KH (1983) Structural kinematics of in-parallel actuated robot arms. J Mech Transm Autom Des 105(4):705–712
12. Gosselin C, Sefrioui J, Richard MJ (1992) Solutions polynomiales au problème de la cinématique des manipulateurs parallèles plans à trois degrés de liberté. Mech Mach Theory 27:107–119
13. Pennock GR, Kassner DJ (1990) Kinematic analysis of a planar eight-bar linkage: application to a platform-type robot. In: ASME proc of the 21th biennial mechanisms conf, Chicago, pp 37–43
14. Gosselin CM, Merlet J-P (1994) On the direct kinematics of planar parallel manipulators: special architectures and number of solutions. Mech Mach Theory 29(8):1083–1097
15. Kong X, Gosselin CM (2001) Forward displacement analysis of third-class analytic 3-RPR planar parallel manipulators. Mech Mach Theory 36:1009–1018
16. Wenger P, Chablat D, Zein M (2007) Degeneracy study of the forward kinematics of planar 3-RPR parallel manipulators. ASME J Mech Des 129:1265–1268
17. Liu X-J, Wang J, Pritschow G (2006) Kinematics, singularity and workspace of planar 5R symmetrical parallel mechanisms. Mech Mach Theory 41(2):145–169
18. Liu X-J, Wang J, Pritschow G (2006) Performance atlases and optimum design of planar 5R symmetrical parallel mechanisms. Mech Mach Theory 41(2):119–144
19. Liu X-J, Wang J, Pritschow G (2006) On the optimal design of the PRRRP 2-DOF parallel mechanism. Mech Mach Theory 41(9):1111–1130
20. Caro S, Chablat D, Wenger P, Angeles J (2003) Isoconditioning loci of planar three-dof parallel manipulators. In: Gogu G, Coutellier D, Chedmail P, Ray P (eds) Recent advances in integrated design and manufacturing in mechanical engineering. Kluwer Academic, Dordrecht, pp 129–138
21. Caro S, Binaud N, Wenger P (2009) Sensitivity analysis of 3-RPR planar parallel manipulators. ASME J Mech Des 131:121005
22. Rakotomanga N, Chablat D, Caro S (2008) Kinetostatic performance of a planar parallel mechanism with variable actuation. In: Advances in robot kinematics, pp 311–320
23. Arakelian V, Briot S, Glazunov V (2008) Increase of singularity-free zones in the workspace of parallel manipulators using mechanisms of variable structure. Mech Mach Theory 43(9):1129–1140

24. Ranjbaran F, Angeles J, Gonzalez-Palacios MA, Patel RV (1995) The mechanical design of a seven-axes manipulator with kinematic isotropy. ASME J Intell Robot Syst 14(1):21–41
25. Al-Sultan KS, Al-Fawzan MA (1997) A tabu search Hook and Jeeves algorithm for unconstrained optimization. Eur J Oper Res 103:198–208
26. Gosselin CM, Angeles J (1990) Singularity analysis of closed-loop kinematic chains. IEEE Trans Robot Autom 6(3):281–290